

Effect of thermal activation energy on dislocation emission from an elliptically blunted crack tip



Xin Zeng, Qi-Hong Fang, You-Wen Liu*

State Key Laboratory of Advanced Design and Manufacturing for Vehicle Body (Hunan University), Changsha, 410082 Hunan Province, PR China

ARTICLE INFO

Article history:

Received 17 March 2014
Received in revised form
11 April 2014
Accepted 21 April 2014
Available online 4 May 2014

Keywords:

Crack
Dislocation
Elliptically blunted crack
Dislocation emission
Thermal activation energy

ABSTRACT

Thermal activation processes are of fundamental importance for the understanding and modeling the strength of structural materials. In this paper, the effect of thermal activation energy on dislocation emission from an elliptically blunted crack tip is researched. Critical stress intensity factors are calculated for an edge dislocation emission from an elliptically blunted crack under mode I and mode II loading conditions at high temperature. The results show that the impact of thermal activation processes is remarkable, the value of the critical stress intensity factor for dislocation emission decreases at high temperature, which means the applied loads for dislocation emission will decrease with increment of temperature.

© 2014 Elsevier B.V. All rights reserved.

1. Introduction

Dislocation emission from a crack tip is one of the most fundamental processes for understanding the ductile–brittle behavior in crystalline materials [1]. An internal back stress due to the dislocations emitted from crack tip accommodates the stress intensity due to applied load, which can increase the fracture toughness of materials [2]. Most of the previous studies supposed that the crack tip is sharp [3–12], but the situation can hardly be observed experimentally [13].

A real crack is always of finite length and the radius of curvature of the crack tip is never small enough to be zero [14,15]. Physically, an atomically sharp crack will be blunted by one atomic plane. It means that the emission of a dislocation from crack tip results in the crack blunting [16,17]. In many previous studies [14,18–21], the image force on an edge dislocation and the critical stress intensity factor for the edge dislocation emission from a blunted crack are calculated. Beltz et al. [22], and Beltz and Fischer [23] found that blunted cracks require a substantially large load to induce dislocation nucleation, whereby a periodic relation is assumed to hold between the shear stress and slip discontinuity along the dominant slip direction ahead of the crack tip [24]. Fischer and Beltz [25] also analyzed the effects of crack blunting on the competition between dislocation nucleation and atomic decohesion.

It is well known that plastic deformation of nanocrystalline and ultrafine-grained metals is thermal activation processes. And thermal activation parameters, such as strain-rate sensitivity exponent and activation volume, depend on temperature and grain size [26–29]. In some previous papers, the effect of thermal activation on dislocation emission from a crack tip was investigated by transition state theory [30–35] and molecular dynamics simulations [36,37]. In this paper, we investigate the effect of thermal activation energy on the emission of edge dislocation from an elliptically blunted crack tip.

When thermal activation processes are analyzed, the applied stress is considered to have two components [38],

$$\tau = \tau_a + \tau^*(T, \dot{\gamma}), \quad (1)$$

where τ is the applied shear stress, τ_a is the long-range internal stress, which is athermal in nature. The thermal component τ^* is called the effective stress and depends on temperature T and shear strain rate $\dot{\gamma}$. The shear strain rate is expressed as an Arrhenius-type rate equation [39–42]

$$\dot{\gamma} = \dot{\gamma}_0 \exp \left[-\frac{G(\tau^*)}{kT} \right], \quad (2)$$

where $\dot{\gamma}_0$ is a pre-exponential factor, $G(\tau^*)$ is the stress-dependent activation energy for the thermal activation dislocation motion, k is the Boltzmann constant.

The main purpose of this paper is to discuss the influence of thermal activation effects on the critical stress intensity factors when edge dislocation is assumed to be emitted from an elliptically blunted crack tip under mode I and mode II loads. And the

* Corresponding author. Tel./fax: +86 731 88822330.
E-mail address: liuyouwu8294@sina.com (Y.-W. Liu).

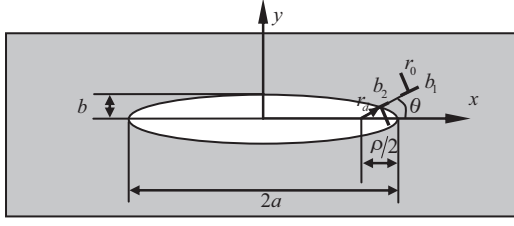


Fig. 1. Dislocation emission from an elliptically blunted crack tip.

critical stress intensity factors for dislocation emission are calculated by using the model of dislocation emission advanced by Lubarda [43].

2. Modeling

Zhang and Li [44,45] calculated the image forces acting on the dislocation which is created by imposing the displacement discontinuity along the cut from a finite-length crack tip to the center of the dislocation, and in the second case, from the center of the dislocation to infinity. Lubarda [43] showed a comparative study of image forces acting on the dislocation which is emitted from the free surface of the void and comes from elsewhere. Then Zeng et al. [46] and Zhao et al. [47] investigated the stress fields of an edge dislocation emitted from the surface of nanovoid with surface effects. In this paper, the stress fields of an edge dislocation emitted from the surface of the elliptically blunted crack are analyzed. As shown in Fig. 1, an infinite elastic medium with the elastic properties ν (Poisson's ratio) and μ (shear modulus) contains an elliptically blunted crack of a the radius of curvature $\rho = b^2/a$. An edge dislocation with Burgers vector b_1 emits from the surface of the blunted crack to the point $z_0 = a - \rho/2 + r_0 e^{i\theta}$, and the other edge dislocation with Burgers vector b_2 locates at the surface of crack $z_d = a - \rho/2 + r_d e^{i\theta}$, where $b_1 = -b_2 = b_x + ib_y = b_r e^{i\theta}$.

Firstly, the associated effective stress component τ^* is considered. The activation energy $G(\tau^*)$ in Eq. (2) can be written as [40]

$$G(\tau^*) = G_0 \left[1 - \left(\frac{\tau^*}{\tau_m} \right)^{p-1} \right]^q, \quad 0 \leq p \leq 1, \quad 1 \leq q \leq 2, \quad (3)$$

where p and q are phenomenological parameters reflecting the shape of a resistance profile, G_0 is the activation energy under the absence of the applied effective stress and τ_m is the effective stress at OK. From Eqs. (2) and (3), we have

$$\tau^* = \tau_m \left\{ 1 - \left[\frac{kT \ln(\dot{\gamma}_0/\dot{\gamma})}{G_0} \right]^{1/q} \right\}^{1/p}. \quad (4)$$

So this equation expresses that the effective stress τ^* depends on the temperature and strain-rate for given G_0 , $\dot{\gamma}_0$, p and q [38].

Then, the effective slip stress τ_m at OK is calculated. According to the work of Nakatani et al. [48], the effective slip stress agrees with Rise's theoretical prediction. The infinite region outside the elliptical blunted crack in the $z = x + iy$ plane is conformally mapped to the infinite region outside a circle of a radius R in the $\zeta = \xi + i\eta$ plane through a transformation function

$$z = \omega(\zeta) = \frac{c}{2} \left(\zeta + \frac{1}{\zeta} \right), \quad (5)$$

where $c = \sqrt{a^2 - b^2}$ and $R = \sqrt{(a+b)/(a-b)}$.

So, the stress fields can be expressed as [49–55]

$$\sigma_y + \sigma_x = 2[\phi'(z) + \overline{\phi'(z)}] = 2[\phi'(\zeta)/\omega'(\zeta) + \overline{\phi'(\zeta)/\omega'(\zeta)}], \quad (6)$$

$$\begin{aligned} \sigma_y - \sigma_x + 2i\tau_{xy} &= 2[\overline{z}\phi''(z) + \psi'(z)] \\ &= 2\omega(\zeta)[\overline{\phi''(\zeta)\omega'(\zeta)} - \phi'(\zeta)\omega''(\zeta)]/[\omega'(\zeta)]^3 + 2\psi'(\zeta)/\omega'(\zeta). \end{aligned} \quad (7)$$

Using Muskhelishvili's complex potential method [56], the complex potential functions in the $\zeta = \xi + i\eta$ plane can be easily calculated as

$$\begin{aligned} \phi(\zeta) &= \gamma \ln(\zeta - \zeta_0) - \gamma \ln(\zeta - \zeta_d) - \gamma \ln(\zeta - R^2/\overline{\zeta_0}) + \gamma \ln(\zeta - R^2/\overline{\zeta_d}) \\ &\quad + \frac{\overline{a_0}\overline{\gamma}R^2}{(\zeta - R^2/\overline{\zeta_0})\overline{\zeta_0}^2} - \frac{\overline{a_d}\overline{\gamma}R^2}{(\zeta - R^2/\overline{\zeta_d})\overline{\zeta_d}^2}, \end{aligned} \quad (8)$$

$$\psi(\zeta) = \chi(\zeta) - \frac{\overline{\omega}(R^2/\zeta)}{\omega'(\zeta)}\phi'(\zeta), \quad (9)$$

$$\begin{aligned} \chi(\zeta) &= \overline{\gamma} \ln(\zeta - \zeta_0) - \overline{\gamma} \ln(\zeta - \zeta_d) - \overline{\gamma} \ln(\zeta - R^2/\overline{\zeta_0}) + \overline{\gamma} \ln(\zeta - R^2/\overline{\zeta_d}) \\ &\quad + \frac{a_0\gamma}{\zeta - \zeta_0} - \frac{a_d\gamma}{\zeta - \zeta_d}, \end{aligned} \quad (10)$$

where $\gamma = \mu b_1/4\pi i(1-\nu)$, $\zeta_0 = (1/c)(z_0 + \sqrt{z_0^2 - c^2})$, $a_0 = ((R^4 + \zeta_0^2)\zeta_0/R^2(\zeta_0^2 - 1)) - (\zeta_0^2(\overline{\zeta_0}^2 + 1)/\overline{\zeta_0}(\zeta_0^2 - 1))$, $\zeta_d = (1/c)(z_d + \sqrt{z_d^2 - c^2})$, $a_d = ((R^4 + \zeta_d^2)\zeta_d/R^2(\zeta_d^2 - 1)) - (\zeta_d^2(\overline{\zeta_d}^2 + 1)/\overline{\zeta_d}(\zeta_d^2 - 1))$.

When the minor semi axis of elliptically crack tends to zero, i.e., $b = 0$, the Eqs. (8 and 9) can be reduced to the solution of a edge dislocation emitted from a finite-length crack tip, which is in accordance with the results of Zhang and Li [45].

According to the Peach–Koehler formula [57], and considering Eqs. (6 and 7), we obtain the image force acting on the dislocation

$$\begin{aligned} f_x - if_y &= [\hat{\tau}_{xy}(z_0)b_x + \hat{\sigma}_y(z_0)b_y] + i[\hat{\sigma}_x(z_0)b_x + \hat{\tau}_{xy}(z_0)b_y] \\ &= (b_x + ib_y)[\hat{\phi}'(z_0) + \overline{\hat{\phi}'(z_0)}] + (b_y - ib_x)[\overline{z_0}\hat{\phi}''(z_0) + \hat{\psi}'(z_0)], \end{aligned} \quad (11)$$

where f_x and f_y are the force in the x and y directions, respectively, $\hat{\sigma}_x(z_0)$, $\hat{\sigma}_y(z_0)$ and $\hat{\sigma}_{xy}(z_0)$ are the components of the perturbation stress fields at the dislocation point z_0 , $\hat{\phi}'(z_0)$ and $\hat{\psi}'(z_0)$ are the perturbation complex potentials in the matrix.

And the perturbation complex potentials are calculated as follows [58]:

$$\begin{aligned} \hat{\phi}'(z_0) &= \left[-\frac{\gamma}{\zeta_0(\zeta_0^2 - 1)} - \frac{\gamma}{\zeta_0 - \zeta_d} - \frac{\gamma}{\zeta_0 - R^2/\overline{\zeta_0}} + \frac{\gamma}{\zeta_0 - R^2/\overline{\zeta_d}} \right. \\ &\quad \left. - \frac{\overline{a_0}\overline{\gamma}R^2}{(\zeta_0\overline{\zeta_0} - R^2)^2} + \frac{\overline{a_d}\overline{\gamma}R^2}{(\zeta_0\overline{\zeta_d} - R^2)^2} \right] / \omega'(\zeta_0), \end{aligned} \quad (12)$$

$$\begin{aligned} \hat{\phi}''(z_0) &= \left\{ \frac{\gamma(2\zeta_0^2 - 1)}{\zeta_0^2(\zeta_0^2 - 1)^2} + \frac{\gamma}{(\zeta_0 - \zeta_d)^2} + \frac{\gamma}{(\zeta_0 - R^2/\overline{\zeta_0})^2} - \frac{\gamma}{(\zeta_0 - R^2/\overline{\zeta_d})^2} \right. \\ &\quad \left. + \frac{2\overline{\zeta_0}\overline{a_0}\overline{\gamma}R^2}{(\zeta_0\overline{\zeta_0} - R^2)^3} - \frac{2\overline{\zeta_d}\overline{a_d}\overline{\gamma}R^2}{(\zeta_0\overline{\zeta_d} - R^2)^3} \right\} - \frac{c}{\zeta_0^3}\hat{\phi}'(z_0) \Big/ [\omega'(\zeta_0)]^2, \end{aligned} \quad (13)$$

$$\begin{aligned} \hat{\psi}'(z_0) &= \left\{ -\frac{\overline{\gamma}}{\zeta_0 - \zeta_d} - \frac{\overline{\gamma}}{\zeta_0 - R^2/\overline{\zeta_0}} + \frac{\overline{\gamma}}{\zeta_0 - R^2/\overline{\zeta_d}} - \frac{\overline{\gamma}}{\zeta_0(\zeta_0^2 - 1)} \right. \\ &\quad \left. + \frac{\gamma\zeta_0^2(\overline{\zeta_0}^2 + 1)}{\overline{\zeta_0}(\zeta_0^2 - 1)^3} + \frac{a_d\gamma}{(\zeta_0 - \zeta_d)^2} - \frac{\gamma(R^4 + 1)(\zeta_0^3 + 3\zeta_0)}{R^2(\zeta_0^2 - 1)^3} \right. \\ &\quad \left. - \frac{\zeta_0(\zeta_0^2 + R^4)}{R^2(\zeta_0^2 - 1)} \left[\frac{\gamma}{(\zeta_0 - \zeta_d)^2} + \frac{\gamma}{(\zeta_0 - R^2/\overline{\zeta_0})^2} - \frac{\gamma}{(\zeta_0 - R^2/\overline{\zeta_d})^2} \right] \right. \\ &\quad \left. + \frac{2\overline{\zeta_0}\overline{a_0}\overline{\gamma}R^2}{(\zeta_0\overline{\zeta_0} - R^2)^3} - \frac{2\overline{\zeta_d}\overline{a_d}\overline{\gamma}R^2}{(\zeta_0\overline{\zeta_d} - R^2)^3} \right] - \frac{\overline{a_0}\overline{\gamma}R^2}{(\zeta_0\overline{\zeta_0} - R^2)^2} \\ &\quad \left. + \frac{\overline{a_d}\overline{\gamma}R^2}{(\zeta_0\overline{\zeta_d} - R^2)^2} \right\} / \omega'(\zeta_0). \end{aligned} \quad (14)$$

The primary physical interest lies on the effective slip stress τ_m which are given by [59]

$$\tau_m = \text{Re}\{i[\hat{\phi}'(z_0) + \overline{\hat{\phi}'(z_0)}] - ie^{2i\theta}[\overline{z_0}\hat{\phi}''(z_0) + \hat{\psi}'(z_0)]\}. \quad (15)$$

Secondly, for the linear elastic analysis of plane cases, Creager and Paris's equations [60] can be used to evaluate the stress fields for an elliptically blunted head. So from Creager and Paris's solutions,

Download English Version:

<https://daneshyari.com/en/article/1809581>

Download Persian Version:

<https://daneshyari.com/article/1809581>

[Daneshyari.com](https://daneshyari.com)